Ferroelectric and Spintronic Devices

Yuan-Chieh Tseng (曾院介)

National Chiao Tung University (NCTU), Taiwan

Distinguished Professor, Dept. Materials Science & Engineering
Associate Vice President, Office of International Affairs
Distinguished Research Fellow, Industrial Technology Research Institute (ITRI)

Part 1: Direct Visualization of Phase Uniformity of ALD-grown $Hf_{1-x}Zr_xO_2$ Ferroelectric Devices

- Phase mapping technique based upon synchrotron x-ray nanobeam
- The technique correlates HZO's microscopic and macroscopic properties.
- New process proposed to optimize HZO, which enabled HZO with a polarization (P_s) value up to 65 μC cm^{-2}; this is the largest P_s ever reported.

Part 2: Failure mode characterizations (experimental & theoretical) for STT- & SOT-MRAM

- Switching failure analysis (transport)
- Micromagnetic simulation for MTJ side-wall (etched) damage
- Micromagnetic simulation for field-free SOT switching
- Atomistic magnetic simulation for damping analysis

Part 3: magneto-electric inverse spin-Hall (MEISH) logic

- Ultra-low energy (atto-joule) operation of the MEISH logic, roadmap of development
- Development of low-voltage-driven multiferroic devices for MEISH

$Hf_{1-x}Zr_xO_2$—potential oxide for NCFET and FTJ

- HZO holds promise for negative capacitance field effect transistors (NCFET) and ferroelectric tunnel junctions (FTJ) due to great compatibility to CMOS technology.
- The FE within HZO originates from the formation of non-centrosymmetric *Pca2₁* orthorhombic phase (O-phase)
- The concern of phase uniformity (**mixed phases of FE & non-FE**) limits HZO towards being fully engaged to the desired technologies.

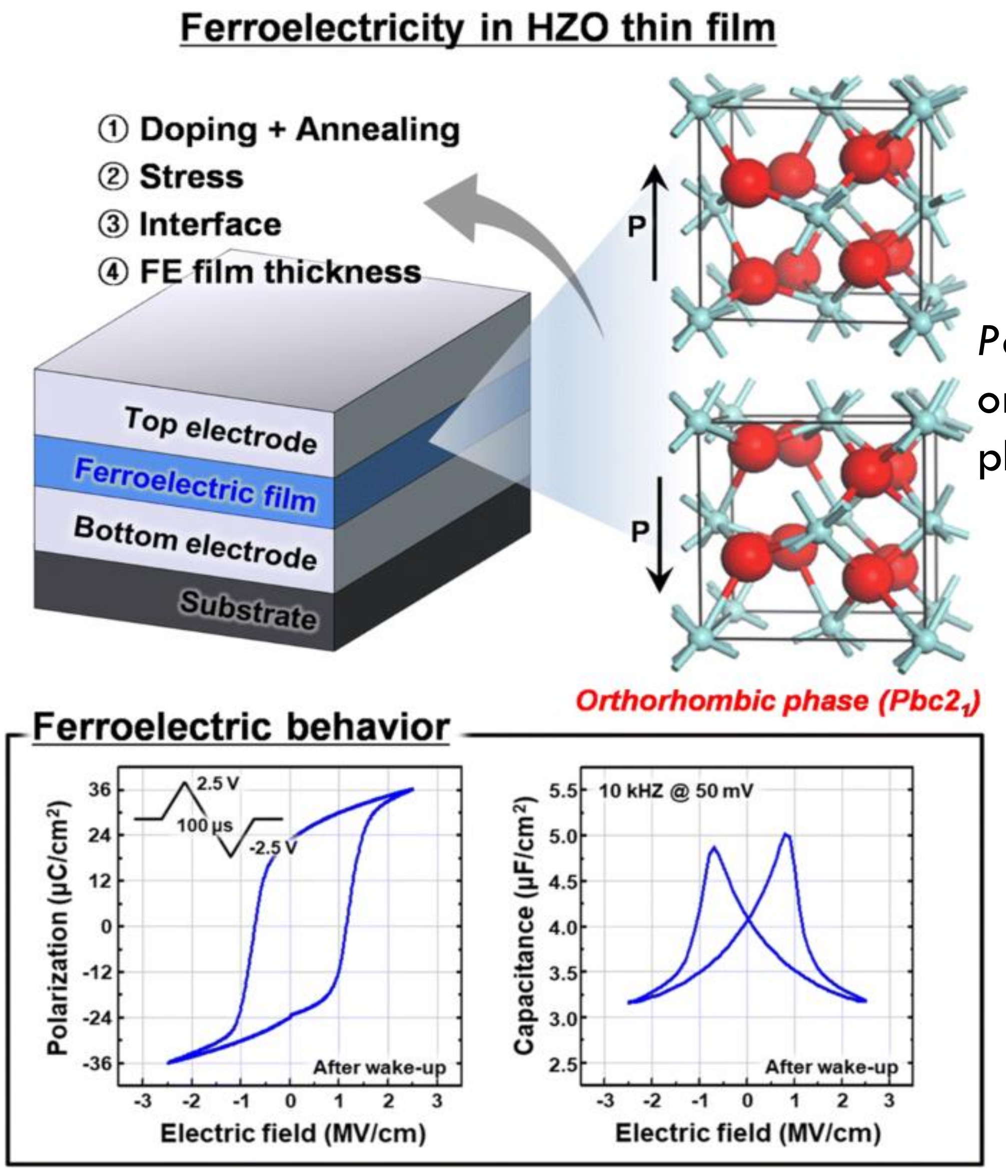

T.S. Böscke et al., *Appl. Phys. Lett.* 99, 102903 (2011)
A. Khan et al., *Nature.* 14, 182 (2015)
X. Wang et al., *Nature Elect.* 3, 440 (2020)

Limitation of X-ray diffraction on HZO phase identification

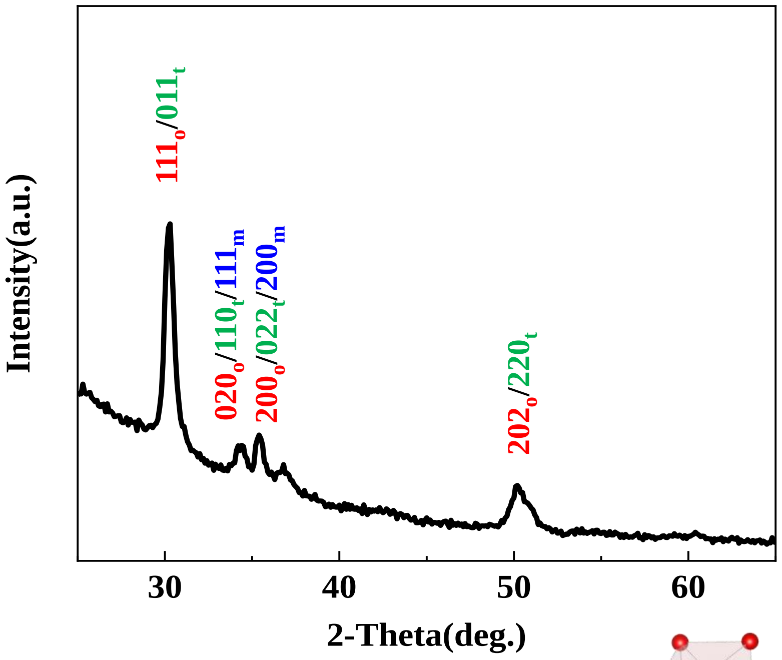

FE

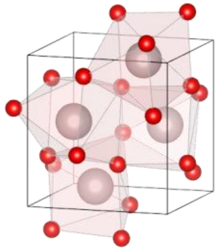

Orthorhombic

DE

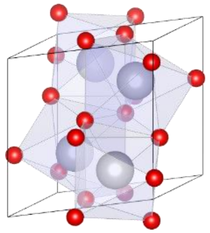

Monoclinic

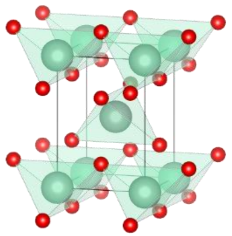

Tetragonal

AFE

- For thin HZO layers in the range of several nanometers (< 5 nm) the FE phase becomes very delicate.
- Phase determination in HZO used to rely on cross-comparison between x-ray diffraction (XRD) and polarization-electric (*P*-*E*) measurements. People use this methodology to examine whether the desired phase is achieved during film optimization.
- XRD is severely constrained to the material's crystalline condition. Structural approach based on XRD easily hits an inherent limit if phase change involves subtle variation in crystallinity for a multiple-phase scenario.

XAFS as a local atomic probe to distinguish multiple phases

XAFS

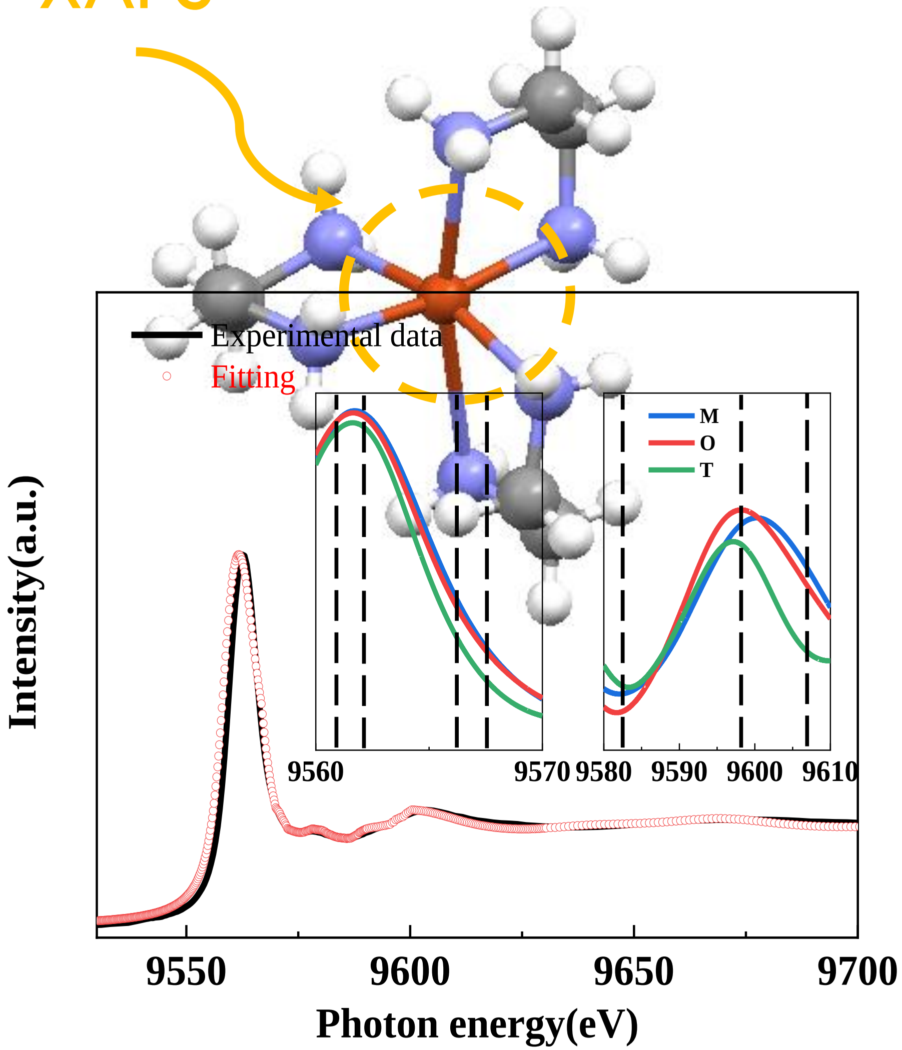

- X-ray absorption fine structure (XAFS) can probe local atomic environment of selected atomic species.
- Crystallinity is not required for XAFS measurements, making it one of the few structural probes available for noncrystalline and highly disordered materials.
- We established theoretical XAFS spectra of the orthorhombic (O), monoclinic (*M*) and tetragonal (*T*) phases separately.
- The three spectra were weighted variably to match the experimental XAFS spectra of the phase-mixed sample.

Mapping based upon XAFS nano-beam

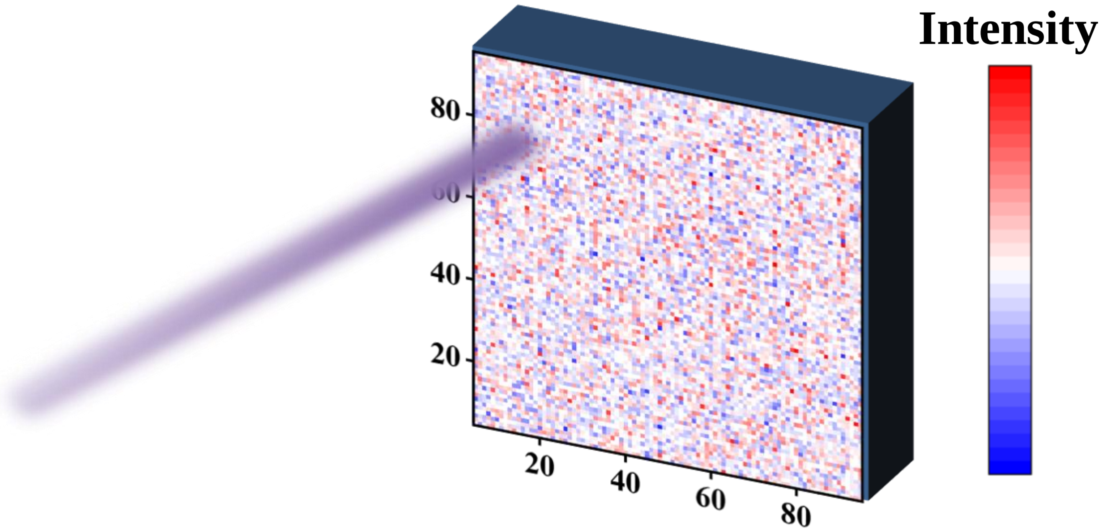

Scanned area: 10um x 10um, spot resolution:100 nm

MOST 科技部 Ministry of Science and Technology

Direct visualization of the multi-phase distribution of HZO

TaN capping on HZO

Mo capping on HZO

TiN capping on HZO

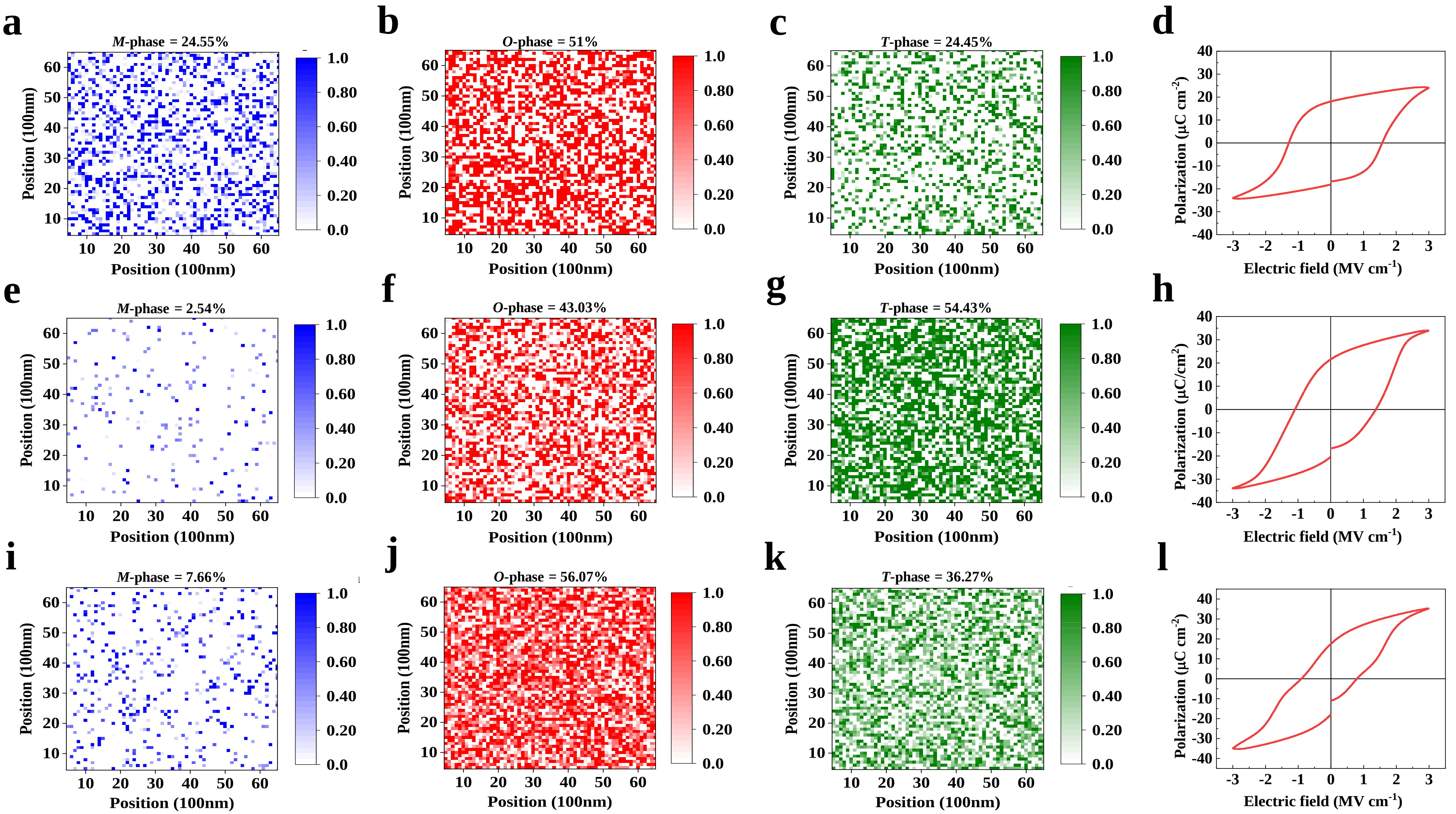

Ferroelectric enhancement based on mapping approach

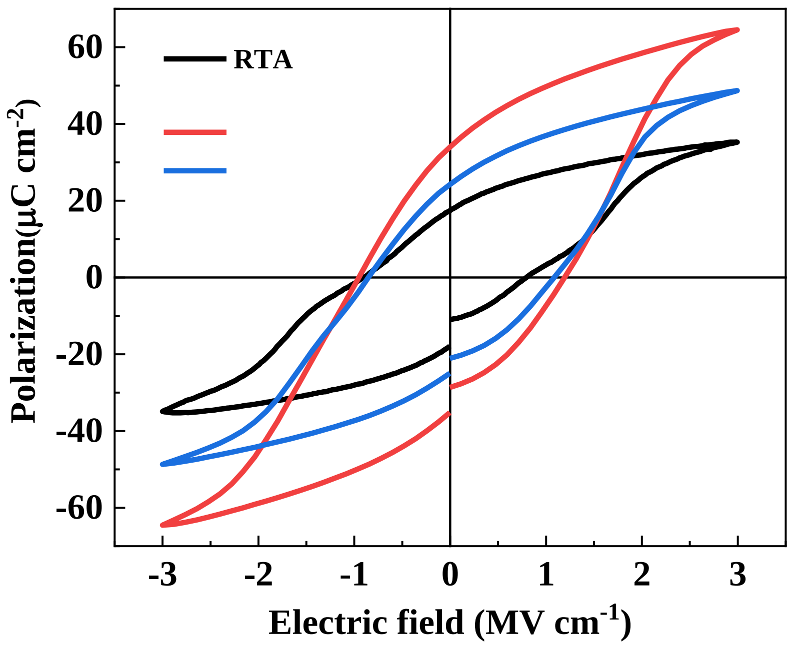

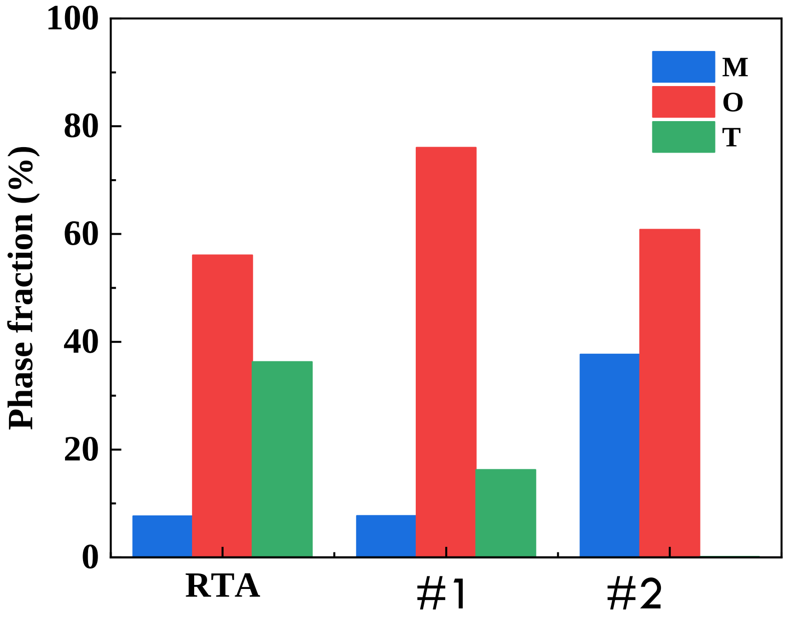

- The mapping technique is very helpful to understand the mode of origin of, as well as the interplay between, the FE and non-FE phases.

- We thus propose new processes (#1,#2) that can enable $H_{0.5}Z_{0.5}O_2$ with a polarization (P_s) value up to ~ 65 μC cm^{-2}. (largest ever reported)

MOST 科技部 Ministry of Science and Technology

Key Drivers for STT (spin-transfer torque) MRAM

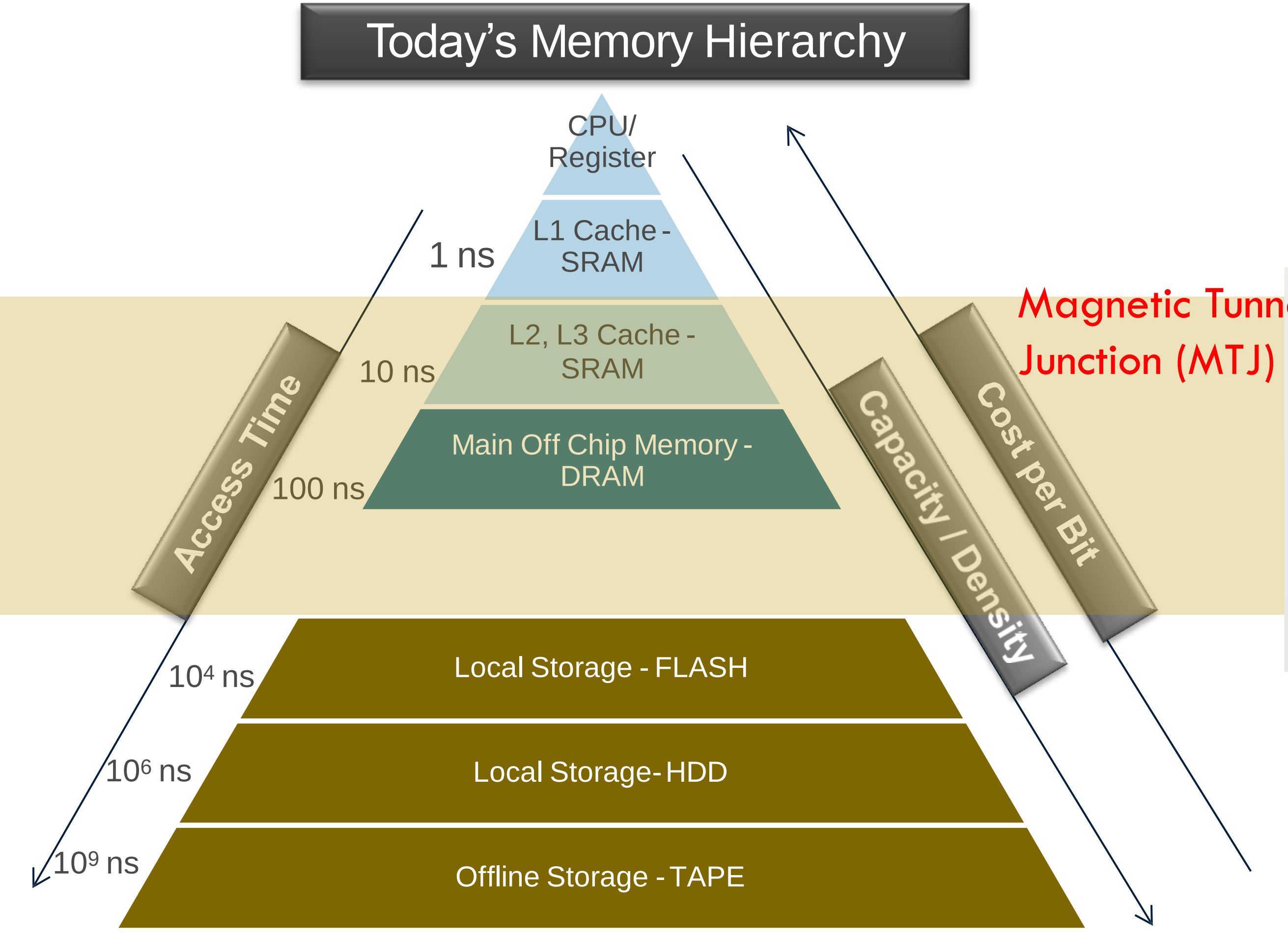

Magnetic Tunnel Junction (MTJ)

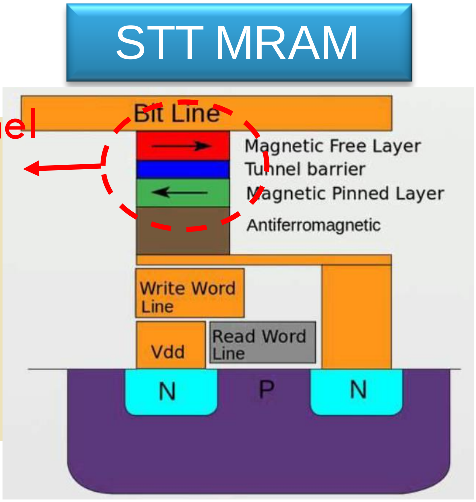

Scaling challenges of current RAM
Latency gap between Storage and RAM

STT (spin-transfer torque) MRAM fabrication and failure analysis

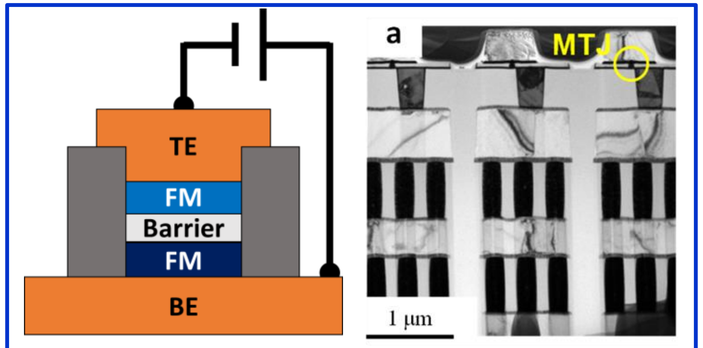

Single pMTJ/CMOS TMR>100%

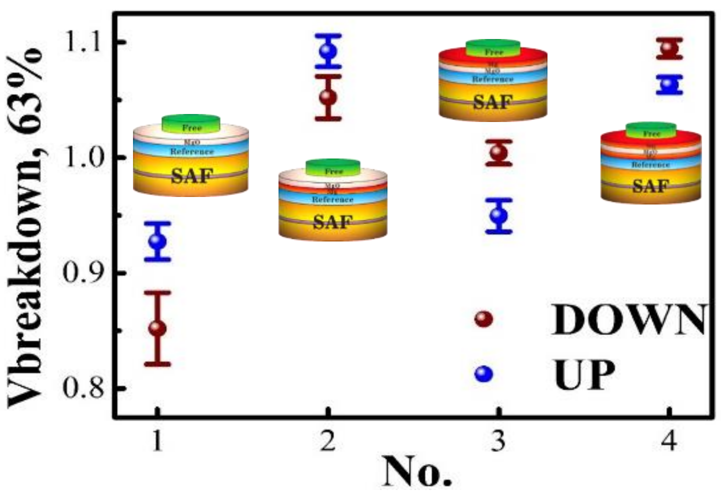

$V_{breakdown}$ v.s. insertion-layer

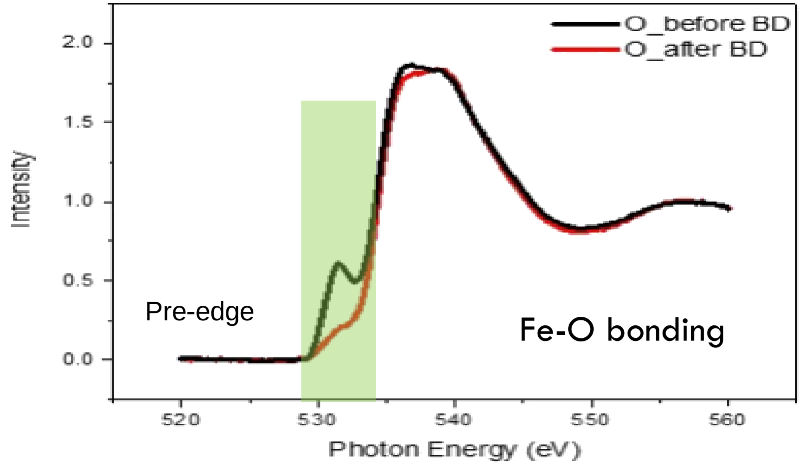

In-situ x-ray to probe breakdown mechanism

MOST 科技部 Ministry of Science and Technology

Switching error analysis and potential applications

◆STT-MRAM write error analysis (Backhopping)

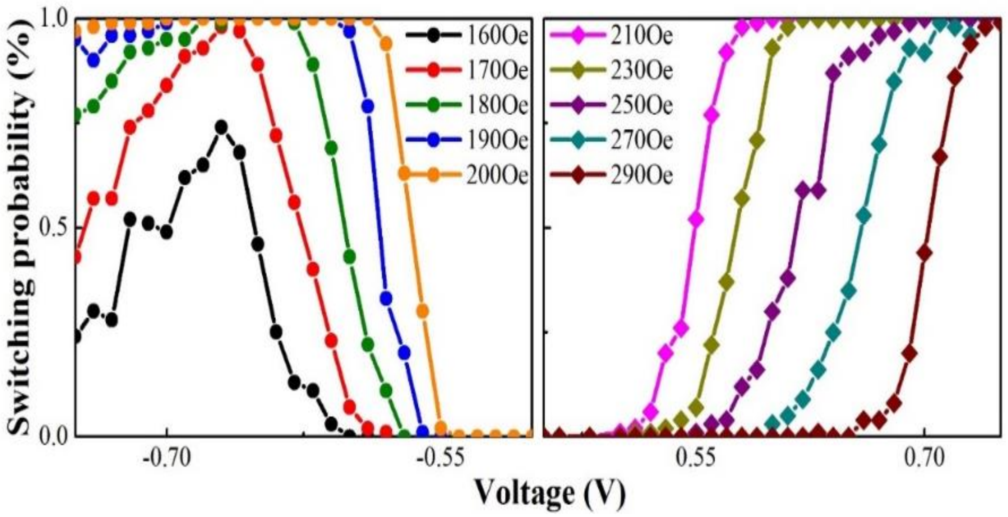

Write error rate increases with increasing V_{appl}.

P/AP
Bi-stable

◆Switching phase diagram (SPD)

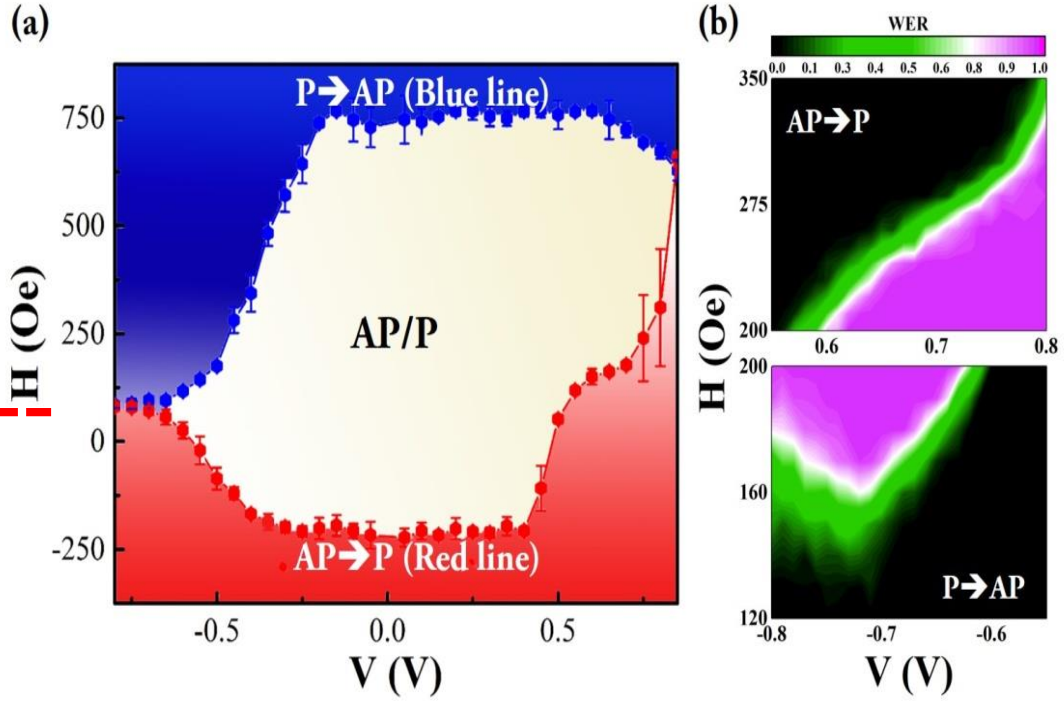

Using SPD to investigate how electrical-magnetic coupling affects switching

With K. M. Chen et al., *Appl. Phys. Lett.* 117, 072405 (2020)

MOST 科技部 Ministry of Science and Technology

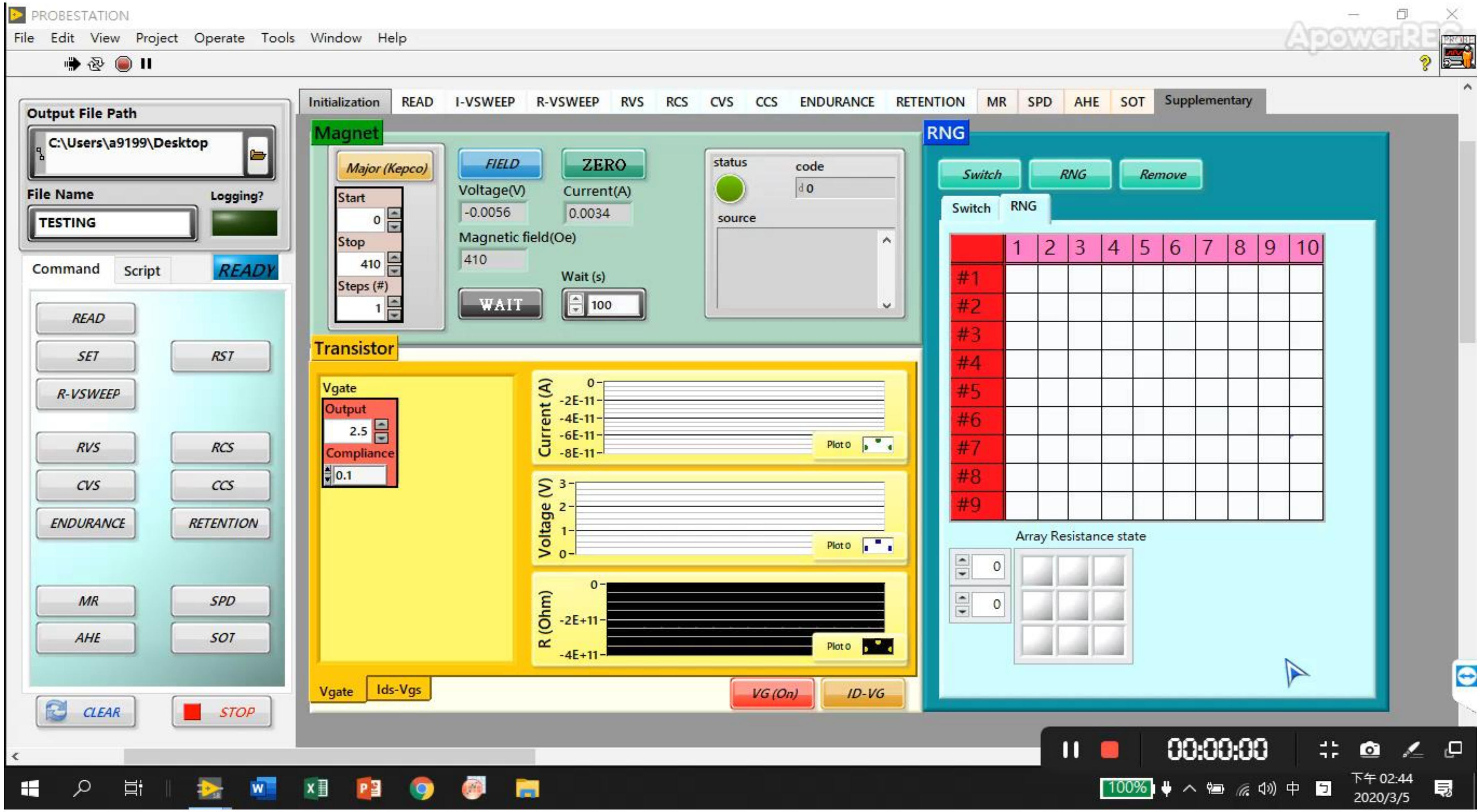

Though the elevated-voltage-induced write error is not good for memory, its fast switching speed with randomness could be potential for neuromorphic computing (application: a random number generator).

Micromagnetic simulation for MTJ side-wall damage effects

Pillar MTJ

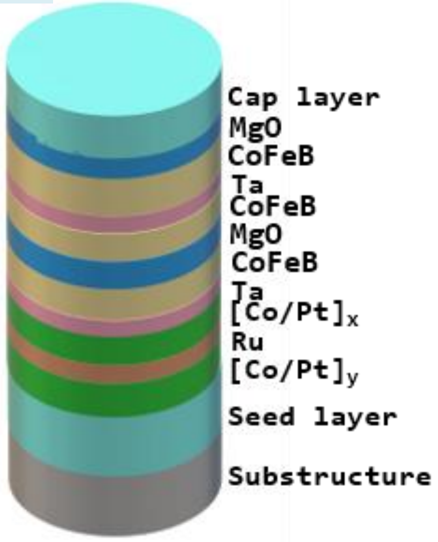

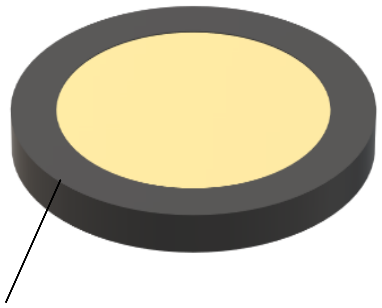

Damaged region (1/10 of the overall region)

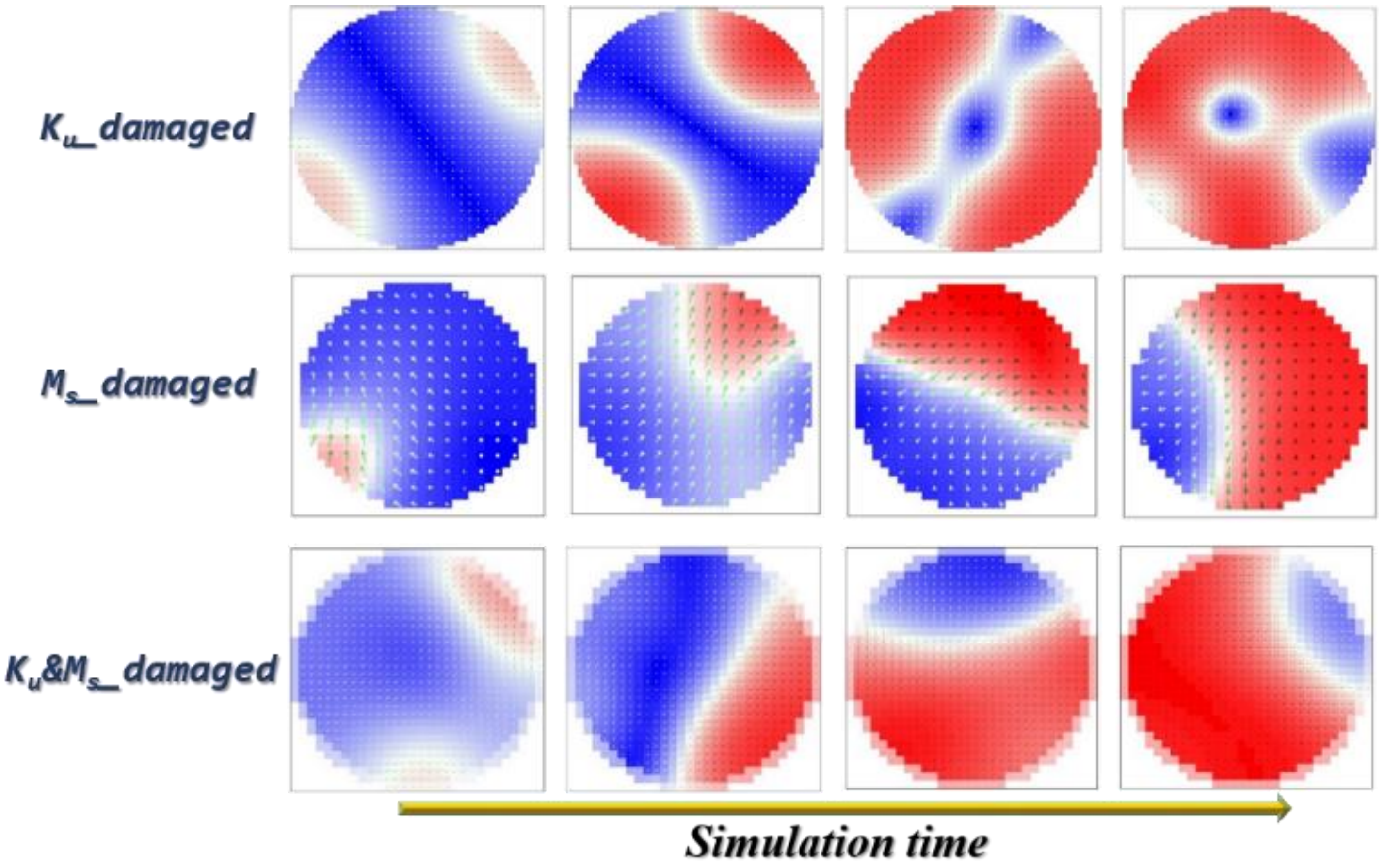

Ku-Ms competition on domain reversal

Prediction of stray field (H_{stary}) and off-set (H_{off}) field effects

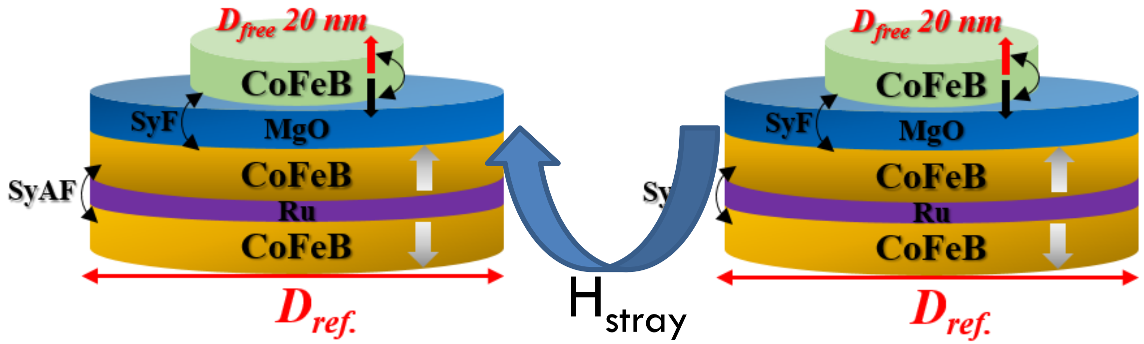

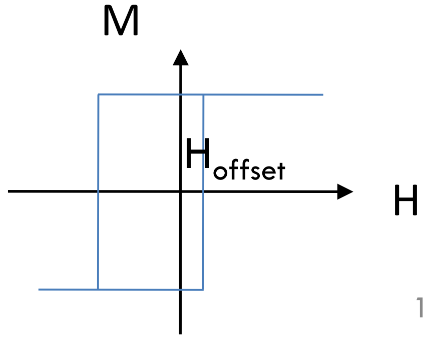

13

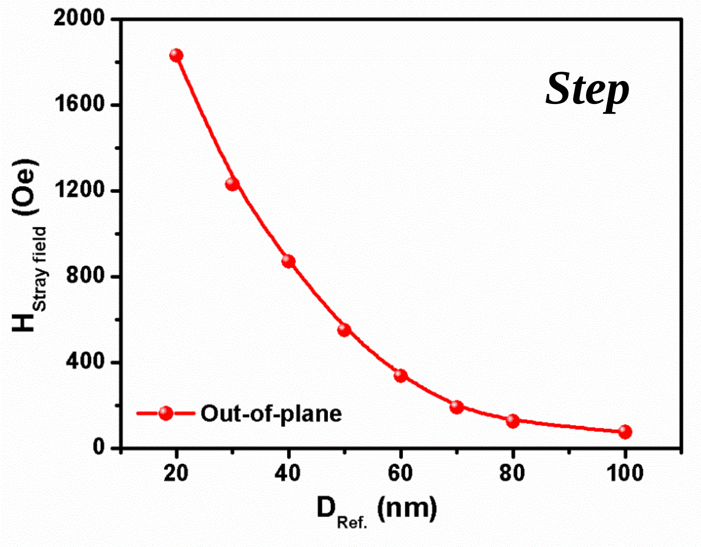

Fixing FL while varying RL size (step structure), H_{stray} appears highly variable.

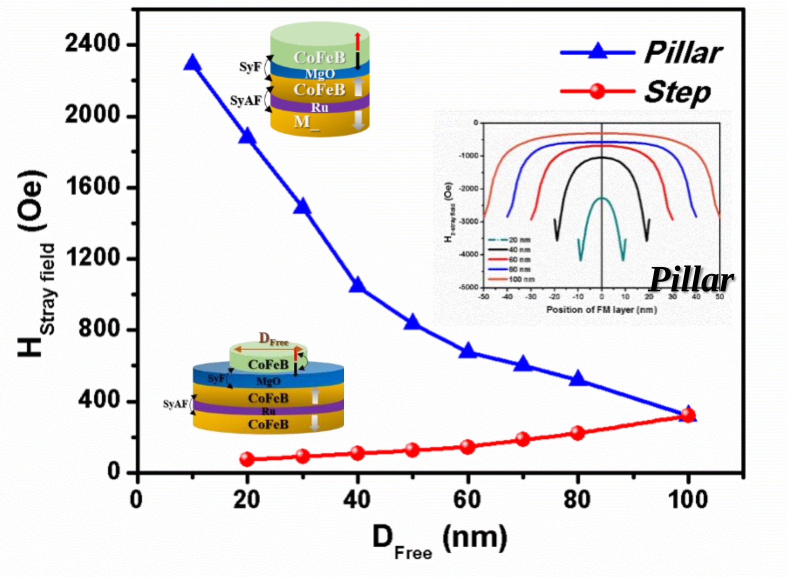

Step MTJ shows more stable H_{stray} compared to pillar MTJ while reducing FL size.

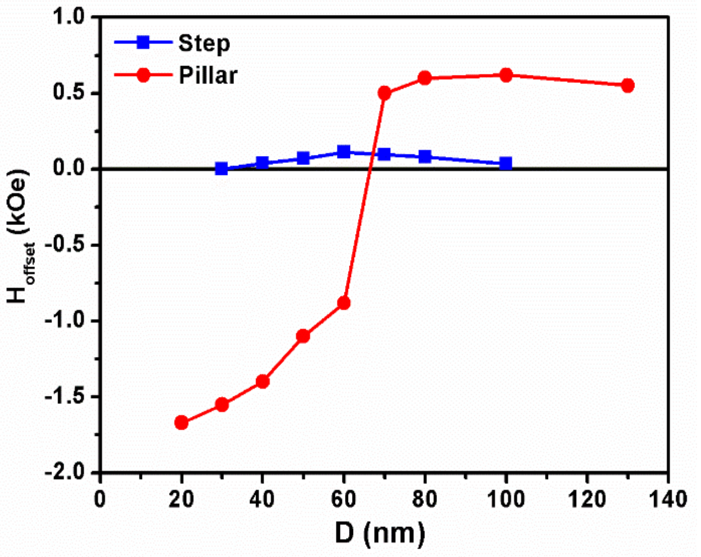

Due to a weaker H_{stary} effect, step MTJ possesses a smaller H_{offset} variation than pillar MTJ while reducing FL size.

Switching simulation for three types of SOT

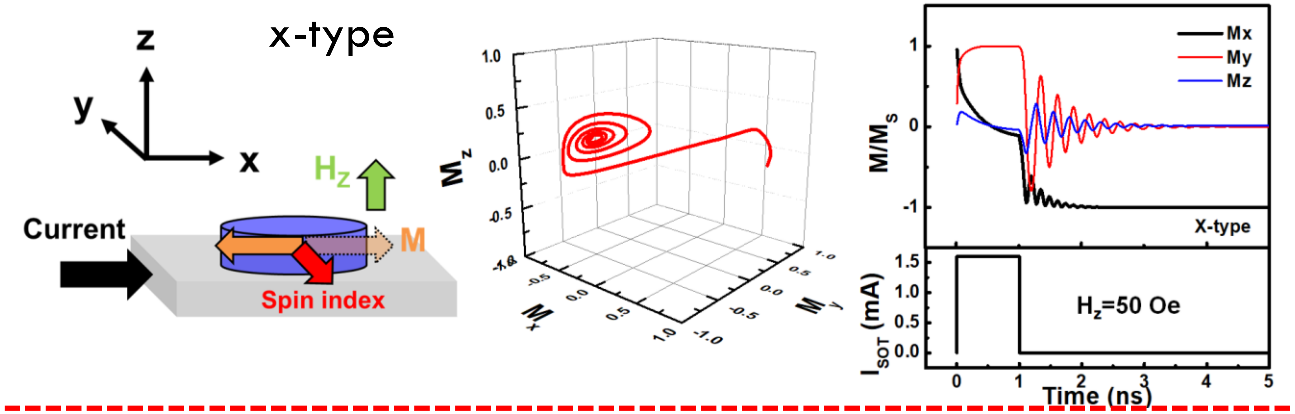

X-type : $H_{external}$ is needed to enable switching

➔ no Incubation delay

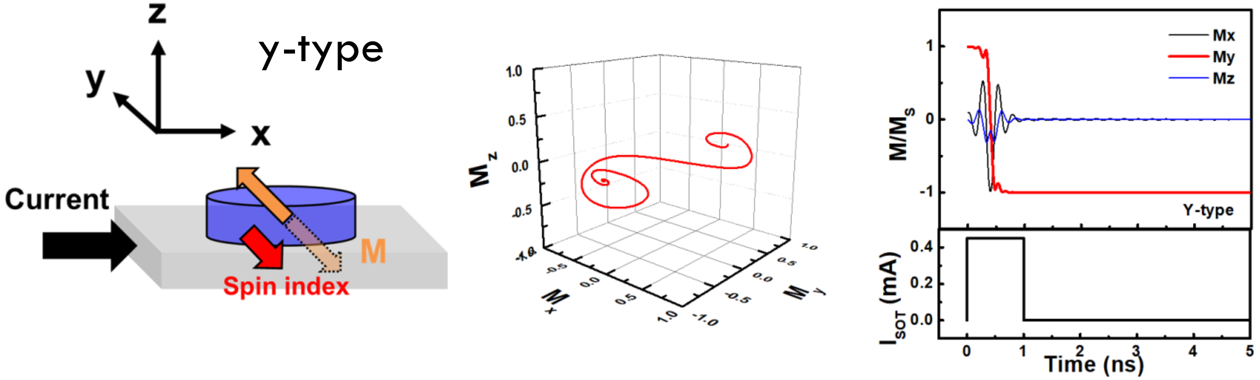

Y-type : switching enabled without $H_{external}$

➔ Incubation delay, lower switching speed

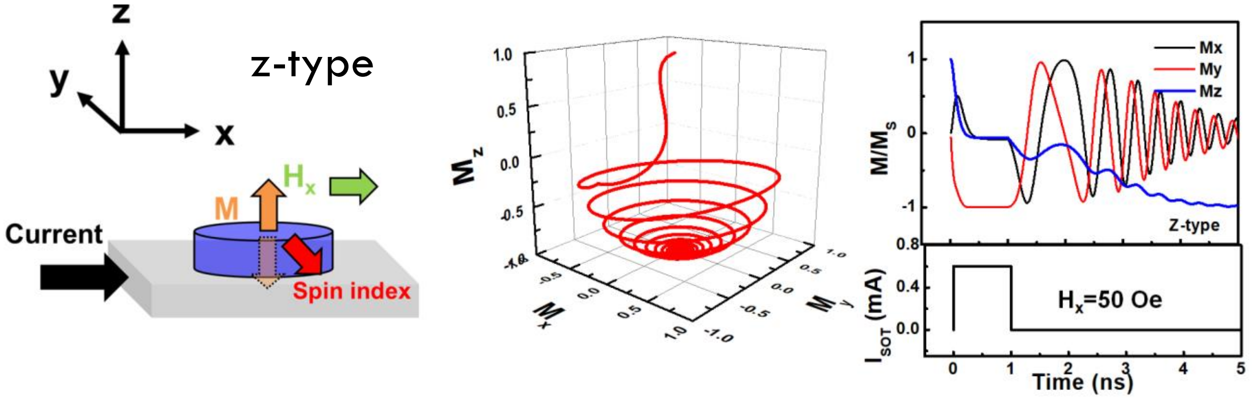

Z-type (**vertical**) : $H_{external}$ is needed to enable switching

➔ no Incubation delay

Z-type SOT switching modeling

The presence of Dzyaloshinskii-Moriya (DM) interaction (intrinsic moment canting either within the layer itself or between layers), may enable "field-free" switching.

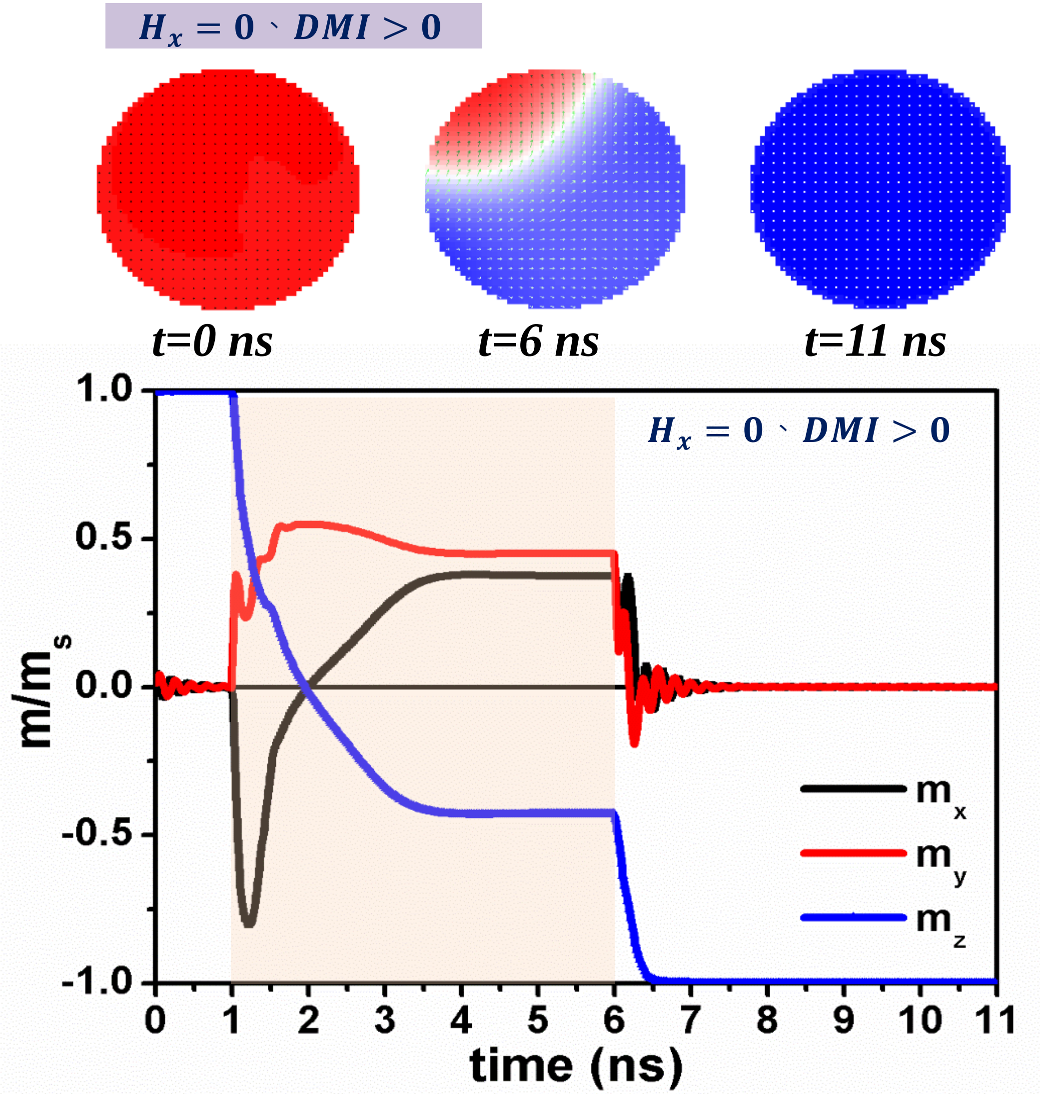

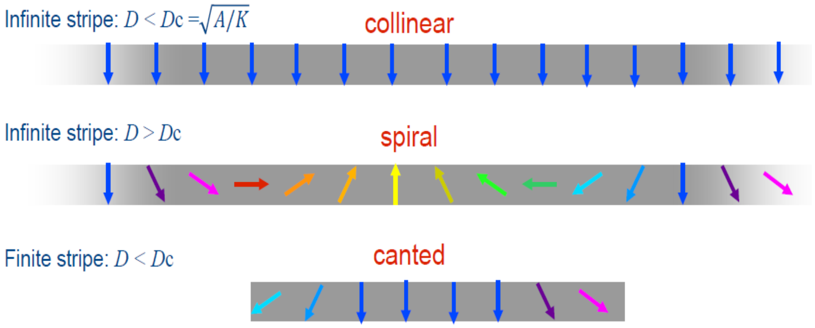

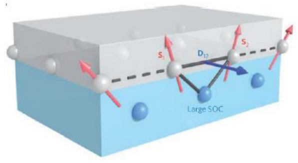

$$H_{DM} = D_{ij}\left(\mathbf{S}_i \times \mathbf{S}_j\right)$$

Device design (stacking, selection of materials)

Manipulating DMI

Field-free switching in Z-type SOT

Atomistic magnetic simulation (Vampire) for SOT

Micromagnetic simulation v.s. Vampire

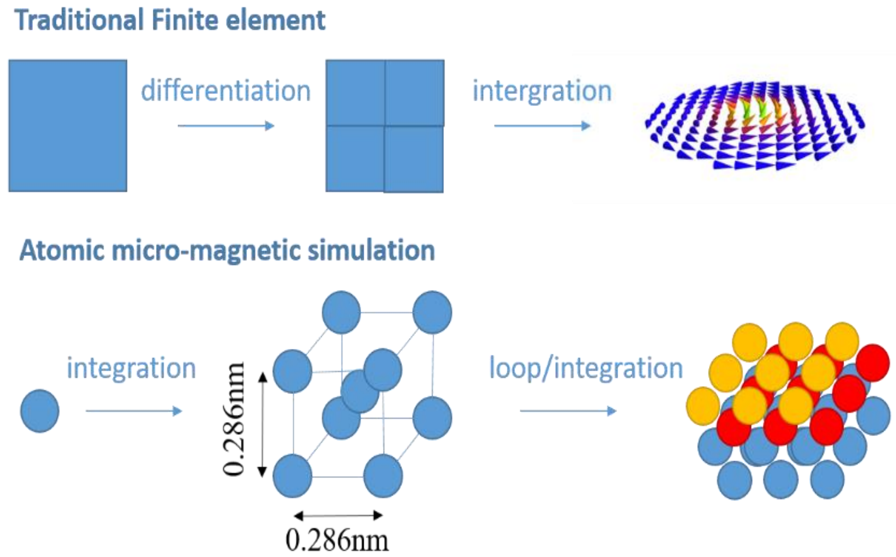

- Directly assign spin to a single atom.
- Atomistic magnetic features for MTJ can be developed, such as interface roughness, defects, etc, which makes simulation closer to real cases!

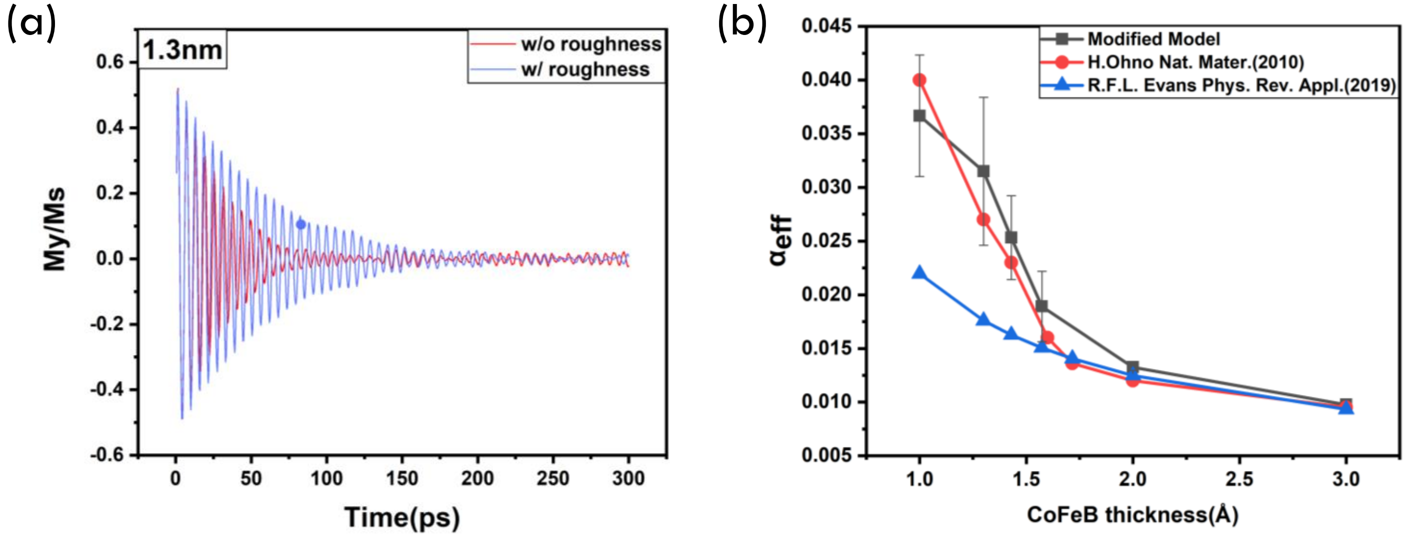

(a) Incorporating interface roughness factor into CoFeB; the damping appears larger

(b) The effective damping (α_{eff}) obtained from Vampire simulation matches the classic reference (Ohno's group, Tohoku Univ. Nature Mater. 9, 721 (2010)) very well!

Magneto-electric inverse spin-Hall (MEISH) logic

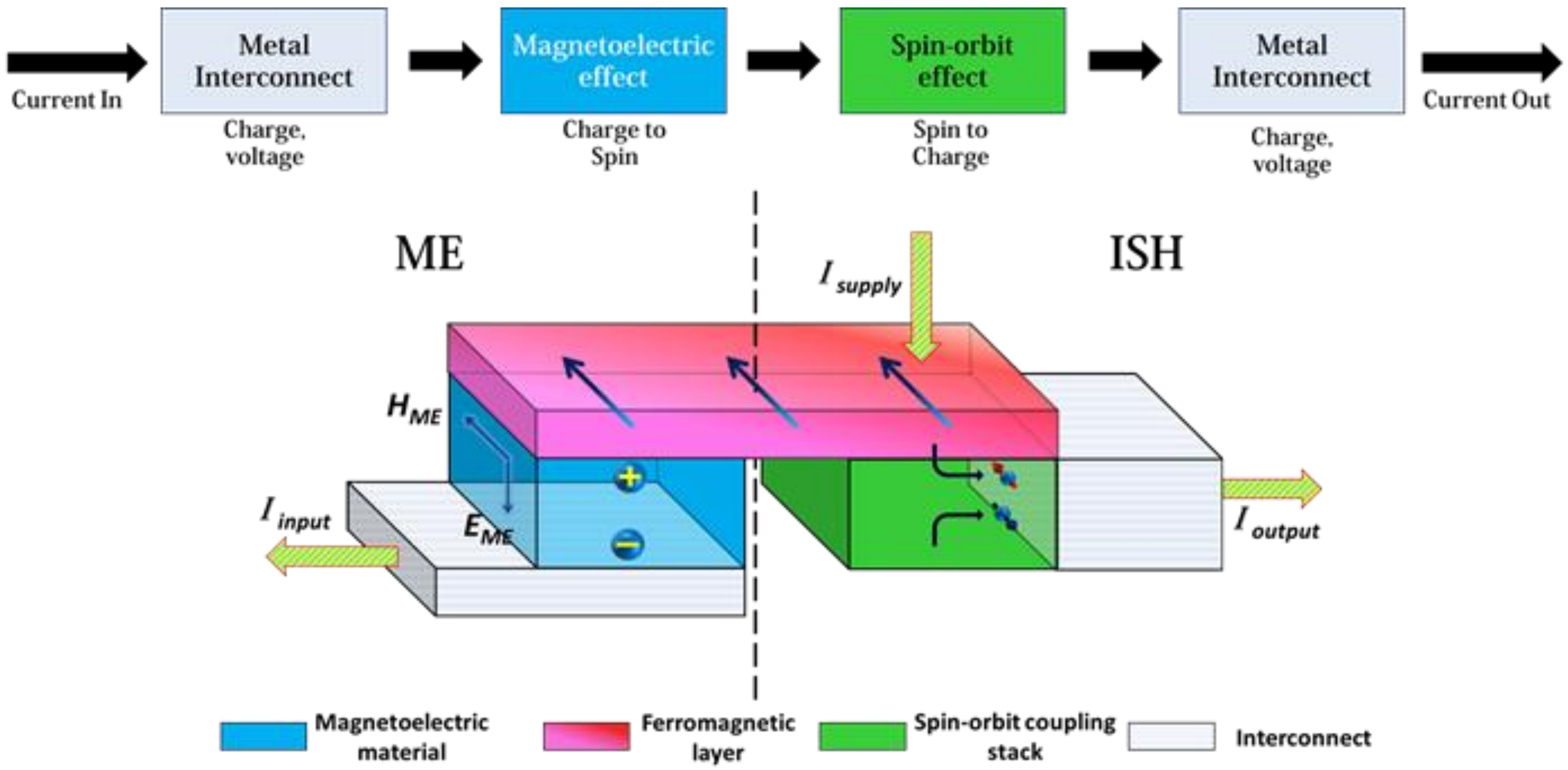

Magnetoelectric inverse spin-Hall (MEISH) device comprises two technologically scalable transduction mechanisms: magnelectric switching and topological conversion of spin to charge (i.e., inverse spin-Hall effect). Our group is committed to develop critical materials related to these two transduction mechanisms.

Roadmap of the MEISH logic development

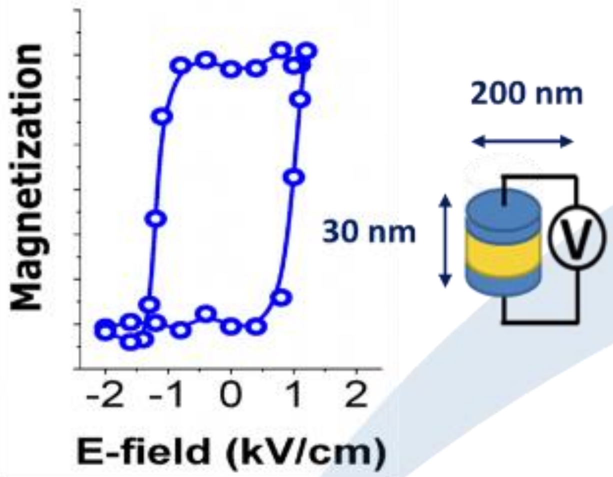

Low-voltage-driven magneto-electrical (ME) capacitor;

candidates: multiferroic systems such as $BiFeO_3$, $GdNi_xFe_{1-x}O_3$

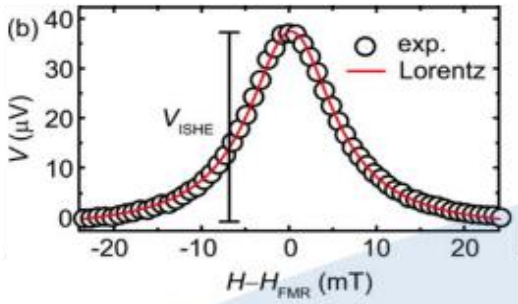

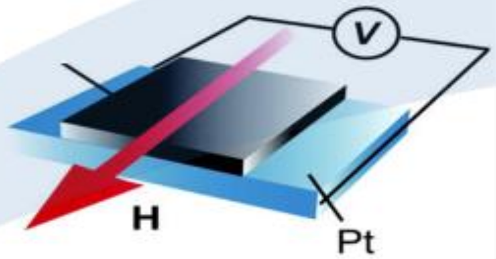

High spin-to-charge conversion inverse-spin-Hall (ISH) systems;

candidates: ferromagnet/topological(Bi_2Se_3) or YIG/noble-metal heterostrutcures.

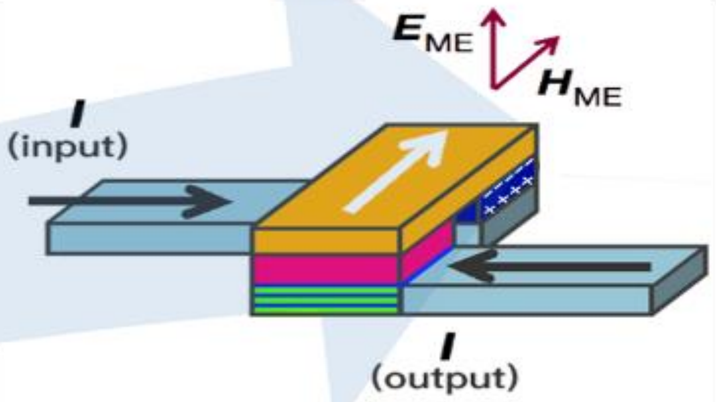

Integration of ME and ISH units to enable a scalable (interconnect <30nm, single cell<100nm), ultra-low energy (<0.1V, atto joule switching) MEISH logic

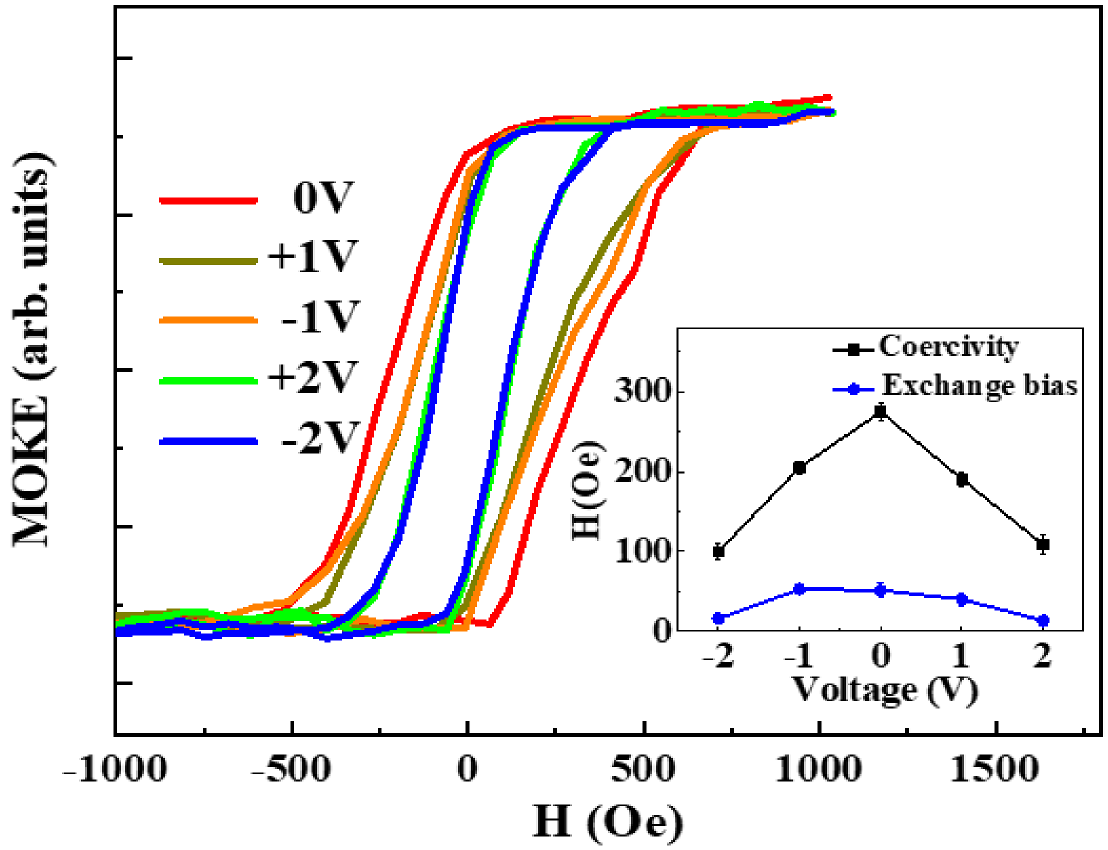

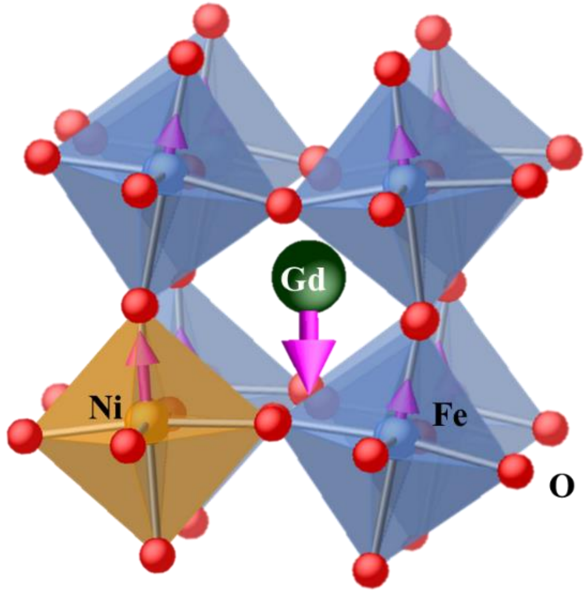

We present a new multiferroic perovskite, $GdNi_xFe_{1-x}O_3$ (GFNO), produced via sputtering on a $SrTiO_3$ substrate. The proposed GFNO is of FE and canted AFM within a monoclinic framework at room temperature, and the magnetic order of the heterostructured device can be controlled very effectively within +/-1 volt.

With S. J. Chang et al., *ACS Appl. Mater. Interf.* 11, 31562 (2019)

Acknowledgement

Dr. C. W. Cheng, Dr. S. J. Chang, K. M. Chen, Y. J. Lin, C. Y. Tang

Prof. C. H. Lai & Dr. C. Y. Yang